Int. J. Electrochem. Sci., 15 **(2020)** 9416 – 9427, doi: 10.20964/2020.09.55

International Journal of
ELECTROCHEMICAL
SCIENCE
www.electrochemsci.org

Characteristics of the YSZ Oxygen Sensor in a Water Content Atmosphere at Elevated Pressures

Guangwei Wang[1,3,*], *Hongzhen Chen*[2,3]

[1] Department of Chemistry and Chemical Engineering, Zunyi Normal University, Zunyi, Guizhou, P. R. China, 563006
[2] Key Laboratory of Ecological Environment and Information Atlas, Fujian Provincial University, Putian, P. R. China, 351100
[3] Chongqing Institute of Green and Intelligent Technology (CIGIT), Chinese Academy of Sciences, Chongqing, P. R. China, 400714
[*]E-mail: wangguangwei@cigit.ac.cn

Received: 30 April 2020 / *Accepted:* 30 June 2020 / *Published:* 10 August 2020

A YSZ oxygen sensor responded correctly to changes in oxygen concentration in an autoclave chamber, although at elevated pressures, the electron transfer numbers agreed well with the theoretical value of 4. The electrochemical impedance spectra (EIS) of the sensor at an oxygen concentration of 500000 ppm, a temperature of 873 K and pressures of 1-80 atm were determined, and those results demonstrated that the overall electrode resistances were strongly dependent on the pressure of the system, which was probably due to the change of physical and chemical characteristics of the working medium. This result is consistent with the strong impact of pressure on the response rate of the oxygen sensor working in a water content atmosphere at elevated pressures.

Keywords: YSZ oxygen sensor, water content atmosphere, elevated pressures, electrochemical impedance spectra

1. INTRODUCTION

Since YSZ solid electrolytes were introduced for in situ pH measurements of a hydrothermal system at elevated temperatures and pressures by Niedrach in the early 1980s [1-2], the in-depth exploration of hydrothermal systems widely existing in natural and industrial processes using in situ electrochemical sensors has attracted great enthusiasm; their introduction opened a new chapter for the development of electrochemical sensors applied to in situ measurements of components and parameters in water content systems with elevated pressures. In the development of these sensors, Hg/HgO/YSZ has been widely used as a reference electrode, and by combining this electrode with another electrode

(e.g., Ag/AgCl, Ag/Ag_2S, Pt(Au)) as the working electrode, electrochemical sensors for pH [3-12], hydrogen sulfide [13-14] and hydrogen [12, 13, 15-17] were established. In addition, using Ag/YSZ as both the reference and working electrodes, an electrochemical "reference system, Ag/YSZ/Ag, aqueous medium" cell was constructed, which exhibited an accurate Nernst response to oxygen in a hydrothermal system [18].

Currently, YSZ-based electrochemical sensors have been successfully applied to the in situ measurements of hydrogen [12, 13], pH [11, 12, 19], hydrogen sulfide [13] and oxygen [20] in various water content systems. However, to further understand the processes that occur in these systems, the sensors need increasingly high accuracy and efficiency. A water content system at high temperature usually has elevated pressure; as a result, the characteristics of YSZ-based sensors working at elevated pressures have received increased attention from researchers.

In this work, the generally applicable Au electrode was used to prepare a "Au/YSZ/Au" electrochemical oxygen sensor, and by assembling the sensor on specially designed experimental equipment, the characteristics of a "Cr-Cr_2O_3, Au/YSZ/Au, water content system" sensor at a temperature of 873 K and pressures ranging from 1 to 80 atm were obtained. The oxygen sensor exhibited a stable response with the alteration of oxygen concentration under the experimental conditions. The impedance spectra of the sensor demonstrated that the overall electrode resistances were strongly dependent on the pressure of the water content system, probably due to the change in the physical and chemical characteristics of the water content medium. In addition, by using the $\Delta\dot{Z}'$ spectra based on the change in pressure, specific pressure-dependent processes were discussed, which play important roles in understanding the electrode reaction mechanisms in water content systems.

2. EXPERIMENTAL PROCEDURE

YSZ tubes were prepared from powders of ZrO_2+8 mol% Y_2O_3 (TOSOH TZ 8Y, Japan) and sintered at 1773 K. After ultrasonic cleaning of the YSZ tubes successively with dilute hydrochloric acid, distilled water and acetone, the Au electrodes on the inside and outside surfaces were prepared using the tape-casting method with Au paste (Kunming Institute of Precious Metals, China) and sintered at 973 K for 2 hours in air. Then, a small drop of Au paste was used to sinter the Au lead on the electrode surfaces at a sintering temperature of 973 K [21-22]. In this study, a Cr-Cr_2O_3 mixture working as the solid oxygen reference system was prepared by filling the mixed powder of Cr and Cr_2O_3 (with a mole ratio of 8:2) carefully inside the tube and subsequently sintering at 973 K for 2 hours in a helium atmosphere. To avoid contact between the solid oxygen reference system and the investigated water content system, the sintered oxygen reference system was isolated from the water content medium using an inorganic insulation material to produce a thin compact sealing film.

The prepared "Au lead, porous Au film/YSZ/porous Au film, Au lead, Cr-Cr_2O_3, inorganic sealing film" device was assembled in an autoclave reactor, with the outside surface completely exposed to the water content system and the inside surface exposed to the solid oxygen reference system of Cr-Cr_2O_3. In this way, a "Cr-Cr_2O_3, Au/YSZ/Au, oxygen gas in the water content system" concentration cell was established, with the outside Au electrode, as the working electrode, having a surface area of

0.64 cm^2 and the inside Au electrode, as the reference electrode, having a surface area of 0.58 cm^2. All of the Au leads were rung out of the autoclave chamber from the metal plug of the autoclave reactor by using inorganic insulation material (Figure 1).

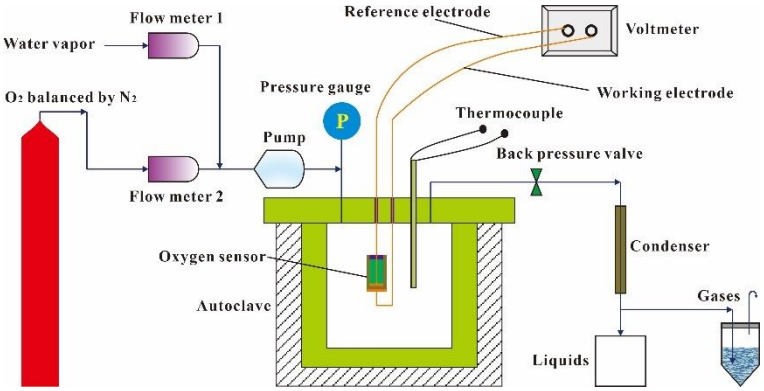

Figure 1. Experimental apparatus for the YSZ oxygen sensor working in a water content system at elevated pressures

The temperature was determined using a NiCr-NiAl thermocouple and could be regulated by a controlling instrument. The pressure in the autoclave chamber was measured using a high-precision digital sensor connected to a gas inlet line with a titanium alloy capillary. By changing the amount of gaseous substances in the chamber, the pressure could be controlled and adjusted. To maintain the pressure in the autoclave chamber, a back valve system was adopted to let the additional gaseous substances leave the reactor. After flowing through a condenser, this discharged fluid was separated into liquids and gases, and then the experimental equipment was left idle. For the detection of the oxygen response of the sensor, the two Au electrodes were contacted with a high-resolution 34410A meter for electromotive force (EMF) measurement. During the electrochemical impedance spectra measurements, the two Au electrodes were connected to the corresponding electrodes of a PAR2263; the signal voltage and frequency range were 50 mV vs. the open circuit potential and 10^6-10^{-3} Hz, respectively.

Prior to each experiment, the autoclave was heated to the test temperature, and a certain volume of gaseous mixture was slowly pumped through the autoclave chamber with a volume flow rate of 100 ml/min. The gaseous mixture was made up of water vapor and oxygen (balanced by nitrogen), and the oxygen concentration was determined by the ratio of oxygen (balanced by nitrogen) and water vapor, which was controlled by flow meters 1 and 2, as presented in Figure 1. According to this experimental apparatus, oxygen response and electrochemical impedance spectra (EIS) of the YSZ oxygen sensor were conducted at temperatures of 873 K and pressures of 1, 20, 40, 60 and 80 atm.

3. RESULTS AND DISCUSSION

3.1 Response of the oxygen sensor

The oxygen response of the "Cr-Cr_2O_3, Au/YSZ/Au, water content system (oxygen gas)" sensor was studied at pressures of 1-80 atm, and the oxygen concentration in the autoclave chamber was

changed successively from 500000 ppm to 200000 ppm, 50000 ppm, 20000 ppm, 5000 ppm, 2000 ppm, 500 ppm, 200 ppm, 500 ppm, 2000 ppm, 5000 ppm, 20000 ppm, 50000 ppm, 200000 ppm and 500000 ppm in sequence. Each experiment started with an oxygen concentration of 500000 ppm and finally returned to that of 500000 ppm. This oxygen concentration of 500000 ppm worked as a base concentration, so the electromotive force of the sensor at this oxygen concentration was defined as E_0. For the convenient comparison of the oxygen response in a water content atmosphere with elevated pressure, ΔE was introduced, which was defined as the difference in the electromotive force at any oxygen concentration compared with E_0 and is presented in equation (1). In Figure 2, the values of ΔE with the alteration of oxygen concentration at different pressures are presented. As shown in Figure 2, the oxygen sensor responded well with the alteration of oxygen concentration in the autoclave chamber. As the oxygen concentration decreased from the base value of 500000 ppm, the ΔE increased. At each oxygen concentration point, ΔE exhibited a stable value, which was determined by the difference in oxygen concentration shown in equation (1). As the oxygen concentration decreased to the lowest value of 200 ppm, the ΔE had the largest value correspondingly. As the oxygen concentration increased from 200 ppm back to the base value of 500000 ppm, ΔE decreased successively and finally almost recovered the starting value of zero. By fitting the ΔE values with the corresponding oxygen concentrations, good linear relationships were obtained. Using the slopes of the fitting lines, the actual electron transfer numbers were computed and are shown in Figure 3. In Figure 3, the actual electron transfer numbers agreed well with the theoretical value of 4. These results indicated that the prepared oxygen sensor has a correct response with the alteration of oxygen concentration, although in an atmosphere containing water and at elevated pressures.

$$\Delta E(\text{Oxygen sensor}) = \frac{RT}{4F} \ln \frac{(P_{O_2})_{\text{other concentration}}}{(P_{O_2})_{500000\ \text{ppm}}} \qquad (1)$$

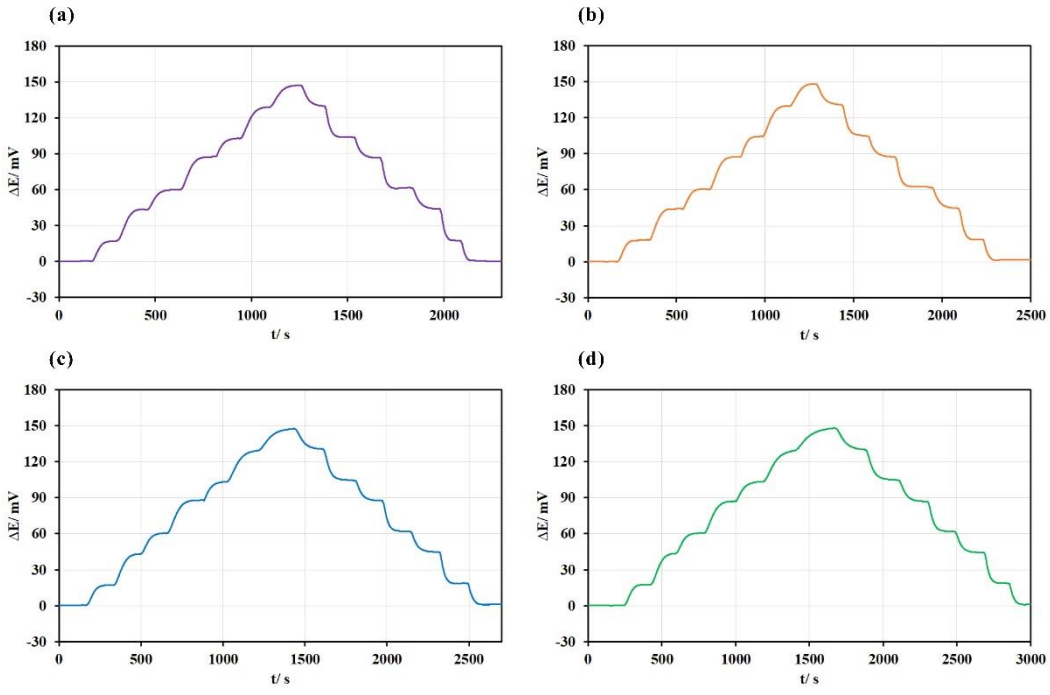

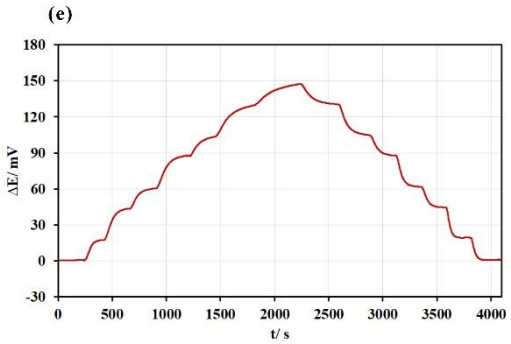

Figure 2. The response (ΔE) of the oxygen sensor as the base oxygen concentration of 500000 ppm was used at a temperature of 873 K and pressures of 1-80 atm, and the oxygen concentration changed successively from 500000 ppm to 200000 ppm, 50000 ppm, 20000 ppm, 5000 ppm, 2000 ppm, 500 ppm, 200 ppm, 500 ppm, 2000 ppm, 5000 ppm, 20000 ppm, 50000 ppm, 200000 ppm and 500000 ppm in sequence. (a): 1 atm; (b): 20 atm; (c): 40 atm; (d): 60 atm; and (e): 80 atm

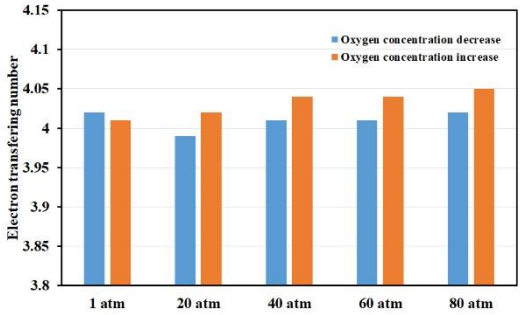

Figure 3. The electron transfer number of the YSZ oxygen sensor in a water content atmosphere at a temperature of 873 K and pressures of 1-80 atm and the oxygen concentration changed successively from 500000 ppm to 200000 ppm, 50000 ppm, 20000 ppm, 5000 ppm, 2000 ppm, 500 ppm, 200 ppm, 500 ppm, 2000 ppm, 5000 ppm, 20000 ppm, 50000 ppm, 200000 ppm and 500000 ppm in sequence.

To study the repeatability of the sensor in the water content atmosphere, it was detected that the oxygen concentration changed successively from 500000 ppm to 200000 ppm, 500000 ppm, 20000 ppm, 500000 ppm, 2000 ppm, 500000 ppm, 200 ppm, 500000 ppm, 2000 ppm, 500000 ppm, 20000 ppm, 500000 ppm, 200000 ppm, and 500000 ppm in sequence, and the corresponding ΔE results at 1 atm and 80 atm are presented in Figure 4. As shown in Figure 4, as the oxygen concentration changed from the base value of 500000 ppm to another value, the ΔE value changed correspondingly. However, as the oxygen concentration changed back to 500000 ppm, the ΔE almost recovered to zero. These results indicated that the sensor exhibited good repeatability in a water content atmosphere, although at elevated pressures up to 80 atm.

To improve the performance of the YSZ-based oxygen sensor, various materials were considered as the reference and sensing electrodes. Konys [23] used Bi-Bi_2O_3 as the oxygen reference in a YSZ oxygen sensor and found that the sensor responds well and can potentially be applied on a large scale. Elyassi [24] prepared a novel YSZ oxygen sensor by using CeO_2-ZrO_2 as the solid-state reference and obtained a satisfactory response in a simulated exhaust gas atmosphere. Adhi [25] adopted Fe-Fe_3O_4 and Bi-Bi_2O_3 as references to prepare YSZ oxygen sensors, and the experimental results indicated that the

sensor outputs have stable cell potentials, which agreed well with the theoretical ones given by the Nernst equation. Compared with the sensor with the Bi-Bi_2O_3 reference, the sensor with the Fe-Fe_3O_4 reference showed a shorter response time. Rivai [26] investigated the performance of a YSZ solid electrolyte oxygen sensor with a Bi-Bi_2O_3 reference electrode and found that the measured EMFs were in good agreement with the theoretical values of the EMF. Iio [27] adopted perovskite-type oxides as a sensing electrode material for a potentiometric YSZ oxygen sensor, which was sensitive to oxygen in a concentration range of 0.05-21% at 600 ℃. The number of electrons for this sensor was approximately 4.2. Miura [28] used Mn_2O_3 as the reference electrode material of a YSZ oxygen sensor and found that the response of the sensor reliably obeys the Nernst equation.

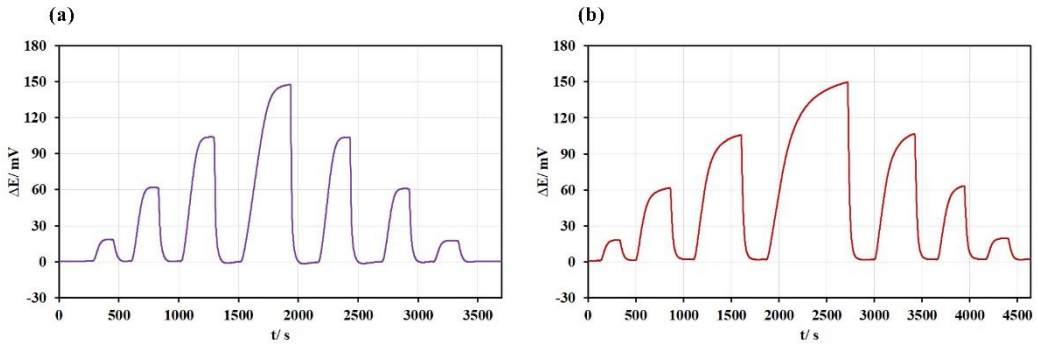

Figure 4. Repeatability of the YSZ oxygen sensor in a water content atmosphere at a temperature of 873 K and pressure of (a): 1 atm; (b): 80 atm. The oxygen concentration changed successively from 500000 ppm to 200000 ppm, 500000 ppm, 20000 ppm, 500000 ppm, 2000 ppm, 500000 ppm, 200 ppm, 500000 ppm, 2000 ppm, 500000 ppm, 20000 ppm, 500000 ppm, 200000 ppm, and 500000 ppm in sequence.

3.2 Electrochemical impedance spectra of the oxygen sensor

According to Figure 2 and Figure 4, the oxygen sensor responded well with the alteration of oxygen concentration in the atmosphere. However, the length of time for each experiment correlated with the pressure of the water content atmosphere. As the pressure increased, the length of time increased. These results indicated that the response rate of the sensor depends heavily on the pressure in the autoclave chamber. To further understand the response rate of the YSZ oxygen sensor at elevated pressures, electrochemical impedance spectra of the sensor at oxygen concentrations of 500000 ppm, temperatures of 873 K and pressures of 1-80 atm were obtained, and the results are presented in Figure 5. As shown in Figure 5, the electrolyte resistances represented by the left intercept of the impedance arc with the real axis are almost unchanged as the pressure is increased from 1 to 80 atm. These results demonstrate the stability of the YSZ electrolyte in the water content system at high pressures. However, the real parts of the impedance spectra corrected for the electrolyte resistances represented by the difference between the right and left intercept of the impedance arc with the real axis, which describes the mass transfer of reactants/products (e.g., absorption, desorption, diffusion, etc.) and charge transfer reactions, are heavily dependent on the pressure in the autoclave chamber.

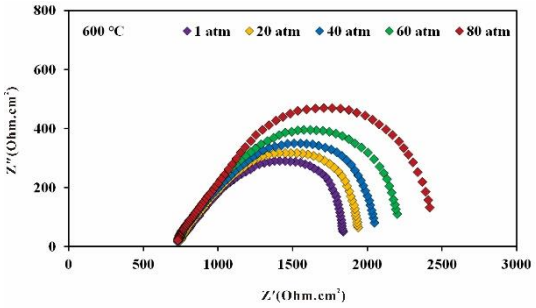

Figure 5. Impedance spectra of the YSZ oxygen sensor in a water content atmosphere at a temperature of 873 K and pressures of 1-80 atm, and the oxygen concentration was 500000 ppm.

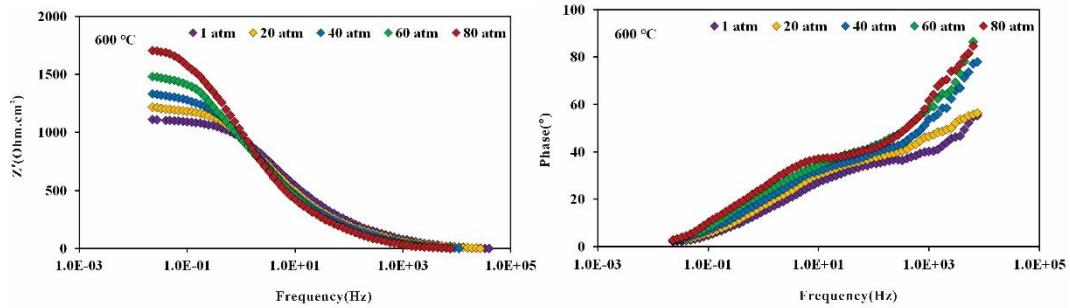

Figure 6. Real part and phase angle of the impedance spectra of the YSZ oxygen sensor in a water content atmosphere corrected for the electrolyte resistances at a temperature of 873 K and pressures of 1-80 atm, and the oxygen concentration was 500000 ppm.

Based on the steady electrolyte resistance, a modified Bode representation can be written as

$$\emptyset = tan^{-1}(\frac{Z_j}{Z_r - R_e}) \quad (2)$$

From equation (2), the phase angle (Φ) corrected for the electrolyte resistance can be calculated. Because the interpretation of the electrode interfacial properties is confounded by the contribution of the electrolyte resistance, the adjusted real part and phase angle are shown in Figure 6.

In Figure 6, the scatter seen in the low frequency of the real part demonstrated the strong impact of pressure on the electrode reactions. Due to the noise in the experimental data, at high frequencies such as $Z_r \rightarrow R_e$, the augmentation to the inverse tangent in equation (2) will have a sign controlled by noise in the denominator, and the phase calculated from equation (2) will have values scattered about Φ (∞). With all of the phase angles lower than 90° at high frequencies, valuable information concerning the existence of CPE behavior that was obscured in the traditional Bode presentation is indicated in Figure 6.

The performance of the "Cr-Cr_2O_3, Au/YSZ/Au, water content system (oxygen gas)" YSZ oxygen sensor applied at high pressures depends on a sequence of processes, such as mass transfer of reactants/intermediates/products, gas-solid reactions, charge transfer reactions, electronic and ionic conduction, etc. Thus, the overall impedance spectrum is a representation of a series of impedance elements describing each process.

$$Z(f) = \sum_i z_i(f) \quad (3)$$

The individual z_i elements may be represented as parallel circuits consisting of several processes. However, relatively small differences or even overlapping phenomenon usually exist in the time constant distribution among individual elements. The parallel connections of impedance elements, such as (RC) circuits, (RQ) circuits, and Gerischer elements, are redundant, and a complete separation into individual elements by means of electrochemical measurement techniques may be impossible.

Here, we use the method introduced by Jensen [29]; according to the change that occurs in an impedance spectrum when the pressure of the system is changed, a new impedance spectrum is yielded by using the spectrum just before such a change and another spectrum just after the change. Hence, it is possible to extract the signal attributed to the pressure change from the sum of elements and selectively detect the pressure contributing to the impedance spectrum.

Now, assume the pressure of the system is changed from condition A to condition B. As a result, a number of impedance elements, z_j, are modified, and a number of impedance elements, z_k, remain constant. Hence, for this change in pressure, the change in Z can be written as

$$\Delta Z = Z|_B - Z|_A \cong \frac{\partial Z}{\partial P}\Delta P = \sum_i \frac{\partial z_i}{\partial P}$$

$$= \sum_j \frac{\partial z_j}{\partial P}\Delta P + \sum_k \frac{\partial z_k}{\partial P}\Delta P = \sum_j \frac{\partial z_j}{\partial P}\Delta P \cong \sum_j (z_{j|B} - z_{j|A}) \quad (4)$$

Then, we define

$$\dot{Z}(f) = \frac{\partial Z(f)}{\partial \ln(f)} \quad and \quad \dot{z}_i(f) = \frac{\partial \dot{z}_i(f)}{\partial \ln(f)} \quad (5)$$

The change in $\dot{Z}$ can then be written as

$$\Delta\dot{Z}(f) = \frac{\partial Z(f)}{\partial \ln(f)}|_B - \frac{\partial Z(f)}{\partial \ln(f)}|_A \cong \sum_j (\dot{z}_{j|B} - \dot{z}_{j|A}) \quad (6)$$

In this work, Z′ is only known for a discrete set of frequencies; for the nth frequency between 2 and n-1, the real part of equation (6) can be rewritten as

$$\Delta\dot{Z}'(f_n) \cong \frac{[Z'_B(f_{n+1}) - Z'_B(f_{n-1})] - [Z'_A(f_{n+1}) - Z'_A(f_{n-1})]}{\ln(f_{n+1}) - \ln(f_{n-1})} \quad (7)$$

where $Z'_A(f_n)$ is the real part of the spectrum in Figure 5 in condition A (1 atm) at frequency f_n and $Z'_B(f_n)$ is the real part of the other spectrum in condition B (20 atm, 40 atm, 60 atm, and 80 atm, respectively.) at f_n. $\Delta\dot{Z}'(f)$ is plotted vs log frequency and is referred to as a $\Delta\dot{Z}'(f)$ spectrum, as shown in Figure 7 (a). By using the circuit shown in Figure 7 (b), the fitted results of the impedance spectrum in Figure 5 were presented in Table 1.

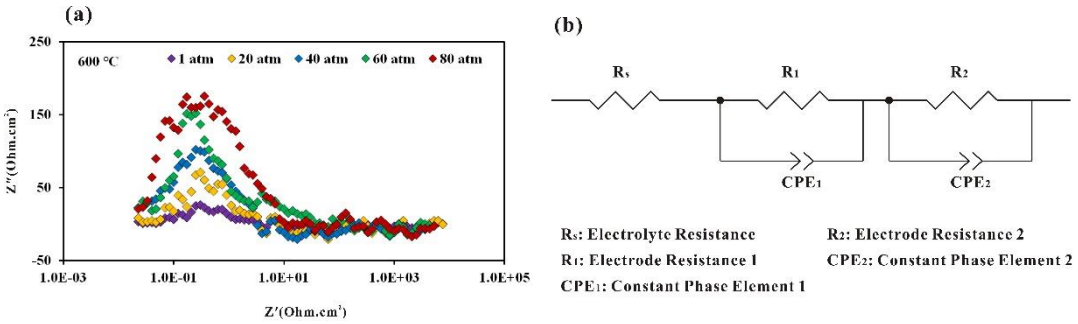

Figure 7. (a) $\Delta\dot{Z}'$ spectra recorded on the YSZ oxygen sensor in a water content atmosphere at a temperature of 873 K and pressures of 1-80 atm. The oxygen concentration was 500000 ppm, and the 1 atm line was a background noise measurement. (b) Equivalent circuit of the studied sensor.

Table 1. Fitting parameters of impedance spectra of the YSZ sensor in a water content atmosphere, at temperature of 873 K and pressures of 1-80 atm, and oxygen concentration was 500000 ppm.

Pressure (atm)	R_s (Ohm.cm^2)	R_1 (Ohm.cm^2)	Q_1 (F)	n_1	R_2 (Ohm.cm^2)	Q_2 (F)	n_1
1	735	376	1.3×10^{-8}	0.83	749	2.5×10^{-8}	0.71
20	738	385	2.9×10^{-8}	0.81	851	2.2×10^{-9}	0.69
40	736	396	6.3×10^{-9}	0.78	942	5.6×10^{-9}	0.68
60	735	405	7.5×10^{-9}	0.79	1115	1.6×10^{-9}	0.65
80	739	408	3.2×10^{-9}	0.75	1354	8.4×10^{-10}	0.68

According to Figure 7 and Table 1, pressure in the autoclave chamber strongly affected the $\Delta\dot{Z}'$ spectra, possibly due to the transfer processes of the active substances, such as oxygen-intermediate transport near the working electrode interfaces, desorption/absorption, disassociation/association, surface diffusion, and ion transfer across the double layer. The reaction mechanism scheme of the "Cr-Cr_2O_3, Au/YSZ/Au, water content system (oxygen gas)" sensors operating in a water content atmosphere at elevated pressures is shown in Figure 8.

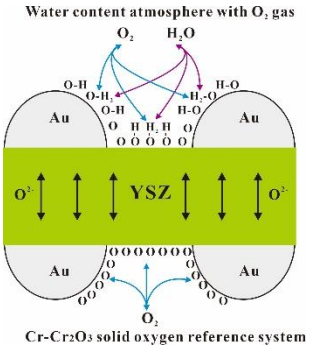

Figure 8. The reaction mechanism scheme of the "Cr-Cr_2O_3, Au/YSZ/Au, water content system (oxygen gas)" sensor in a water content atmosphere at high pressures

On the working electrode, water molecules may be absorbed on the electrode interfaces by physisorption and chemisorption via chemical bonds and van der Waals forces, respectively [30]. At the "Au/YSZ/water content atmosphere" boundary, the absorbed water molecules can disassociate into hydrogen ions and hydroxide ions; these ions and the oxygen atoms originating from the oxidation reaction of oxygen ions may be converted into hydroxide ions, water molecules and other intermediates. The most likely transfer paths for these electroactive intermediates to depart from the boundary are ① desorption into the water content atmosphere; ② spreading into the "Au/water content atmosphere" interface followed by desorption; and ③ spreading into the "YSZ/water content atmosphere" interface followed by desorption.

Similarly, numerous electroactive intermediates were formed at the Au/YSZ interface, and there are two probable routes for these components to be transferred: entry into the bulk electrode via site-exchange reaction with Au atoms [31-32] or spreading to the three phase boundary (TPB) and mixing with the electroactive intermediates yielded there.

On the surface of the YSZ, hydrogen ions can react with oxygen ions to form hydroxide ions [33]. However, due to the weak electroconductivity of YSZ, the oxidation of oxygen ions on the surface is strongly limited.

The diffusion coefficient of electroactive intermediates in the autoclave chamber can be estimated using the following empirical formula with an applicable pressure range of 1 to 25 atm [34-35].

$$D_{AB} = \frac{0.001858T^{1.5}}{P\sigma_{AB}^2\Omega_D}\left(\frac{1}{M_A}+\frac{1}{M_B}\right)^{1/2} \quad (8)$$

where D_{AB} is the mass diffusivity of electroactive intermediates in the water content medium, in cm^2/s; T is the absolute temperature, in K; M_A and M_B are the molecular weights of electroactive intermediates and water, respectively; P is the absolute pressure, in MPa; σ_{AB} is the "collision diameter," a Lennard-Jones parameter, in Å; and Ω_D is the "collision integral" for molecular diffusion, a dimensionless function of the temperature and the intermolecular potential field for one molecule of electroactive intermediates and one molecule of water.

Above 25 atm, the effect of viscosity resulting from density alteration must be considered beyond equation (8). Because the volume of the chamber is defined, the density of substances increases with increasing pressure, which results in the augmented dynamic viscosity of the water content medium. For a good approximation, the diffusivity of the species depended on the pressure to a larger extent compared with the common inverse relationship in equation (8) [7]. Similarly, together with the strong dependence on the temperature observed in equation (8), the diffusivity of electroactive intermediates is additionally strengthened by the change in viscosity resulting from the density alteration.

These characteristics are in good correspondence with the strong dependency of gas diffusion processes on the pressure of the water content system, which are represented by the peaks in the $\Delta\dot{Z}'$ spectra.

According to the Langmuir equation, the chemical and physical absorption of active substances at the electrode interfaces can be expressed as [36-37].

$$\frac{\theta_{ch}}{1-\theta_{ch}} = PK_0\exp\left(\frac{Q_{ch}}{kT}\right) \qquad Q_{ch} > 0 \quad (9)$$

$$\frac{\theta_{ph}}{1-\theta_{ph}} = PK_0 \exp\left(\frac{Q_{ph}}{kT}\right) \qquad \mathrm{Q_{ph}} > 0 \qquad (10)$$

where θ is the relative coverage, P is the pressure, K_0 is a constant, k is the Boltzmann constant, T is the temperature, and Q is the enthalpy for absorption of water. Equations (9) and (10) demonstrate that the absorption of active substances is not only temperature-dependent but also pressure-dependent.

As the pressure increased from 1 to 80 atm, numerous hydroxide and hydrogen ions were generated and absorbed on the electrode interfaces. Thus, the absorption and diffusion of electroactive species are substantially limited due to the occupation of the majority of absorbing sites. Because of these kinds of gas-solid reactions (dissociation and absorption of water molecules, occupation of the absorption sites, diffusion/absorption/desorption of electroactive species on the electrode interfaces), the peak on the $\Delta\dot{Z}'$ spectra depends strongly on the pressure of the water content system. This result is consistent with the strong impact of pressure on the response rate of the oxygen sensor working in a water content atmosphere at elevated pressures.

4. CONCLUSIONS

The YSZ oxygen sensor responded correctly o the changes in oxygen concentration in the autoclave chamber, although at elevated pressures, the electron transfer numbers agreed well with the theoretical value of 4. Electrochemical impedance spectra (EIS) of the sensor at an oxygen concentration of 500000 ppm, a temperature of 873 K and pressures of 1-80 atm were determined, and they demonstrated that the overall electrode resistances are strongly dependent on the pressure of the system, which was probably due to the change of physical and chemical characteristics of the working medium. This result is consistent with the strong impact of pressure on the response rate of the oxygen sensor working in a water content atmosphere at elevated pressures.

ACKNOWLEDGEMENTS

This work was financially supported by the National Natural Science Foundation of China (No. 41763008), the Natural Science and Technology Foundation of the Guizhou Provincial Department of Education (No. [2017]086), the Natural Science and Technology Foundation of Guizhou Province (No. [2019]1461), the Technologies R & D Program of Guizhou Province (No. [2018]2774), the Doctor Foundation of Zunyi Normal University (Zunshi BS [2017]02), and the Open Funding of Key Laboratory of Ecological Environment and Information Atlas (ST18002).

References

1. L. W. Niedrach, *J. Electrochem. Soc.*, 127 (1980) 2122.
2. L. W. Niedrach, *Sci.*, 207 (1980) 1200.
3. T. Tsuruta and D. D. Macdonald, *J. Electrochem. Soc.*, 129 (1982) 1221.
4. S. Hettiarachchi and D. D. Macdonald, *J. Electrochem. Soc.*, 131 (1984) 2206.
5. S. Hettiarachchi, P. Kedzierzawski and D. D. Macdonald, *J. Electrochem. Soc.*, 132 (1985) 1866.
6. D. D. Macdonald, S. Hettiarachchi, H. Song, K. Makela, R. Emerson and M. Haim, *J. Solution*

Chem., 21 (1992) 849.
7. D. D. Macdonald and L. B. Kriksunow, *Electrochim. Acta*, 47 (2001) 775.
8. M. J. Danielson, O. H. Koski and J. Myers, *J. Electrochem. Soc.*, 132 (1985) 296.
9. M. J. Danielson, O. H. Koski and J. Myers, *J. Electrochem. Soc.*, 132 (1985) 2037.
10. S. N. Lvov, X. Y. Zhou, G. C. Ulmer, H. L. Barnes, D. D. Macdonald, S. M. Ulyanov, L. G. Benning, D. E. Grandstaff, M. Manna and E. Vicenzi, *Chem. Geol.*, 198 (2003) 141.
11. K. Ding, Jr W. E. Seyfried, Z. Zhang, M. K. Tivey, K. L. V. Damm and A. M. Bradley, *Earth Planet. Sc. Lett.*, 237 (2005) 167.
12. K. Ding, Jr W. E. Seyfried, *Chem. Rev.*, 107 (2007) 601.
13. K. Ding, Jr W. E. Seyfried, M. K. Tivey and A. M. Bradley, *Earth Planet. Sci. Lett.*, 186 (2001) 417.
14. R. H. Zhang, X. T. Zhang and S. M. Hu, *Sens. Actuators, B*, 177 (2013) 163.
15. K. Ding and Jr W. E. Seyfried, *Geochim. Cosmochim. Acta*, 59 (1995) 4769.
16. K. Ding and Jr W. E. Seyfried, *J. Solution Chem.*, 25 (1996) 421.
17. R. H. Zhang, S. M. Hu and X. T. Zhang and Y. Wang, *Anal. Chem.*, 80 (2008) 8807.
18. N. Hara and D. D. Macdonald, *J. Electrochem. Soc.*, 144 (1997) 4158.
19. L. Manjakkal, D. Szwagierczak, R. Dahiya, Prog. Mater. Sci., 109 (2020) 100635.
20. T. Liu, X. Zhang, L. Yuan, J. Yu, *Solid State Ionics*, 283 (2015) 91.
21. A. Jaccoud, G. Fóti and Ch. Comninellis, *Electrochim. Acta*, 51 (2006) 1264.
22. A. Jaccoud, G. Fóti, R. Wüthrich, H. Jotterand and Ch. Comninellis, *Top. Catal.*, 44 (2007) 409.
23. J. Konys, H. Muscher, Z. Voß, O. Wedemeyer, J. Nucl. Mater., 335 (2004) 249.
24. B. Elyassi, N. Rajabbeigi, A. Khodadadi, S. S. Mohajerzadeh, M. Sahimi, *Sens. Actuators, B,* 103 (2004) 178.
25. P. M. Adhi, M. Kondo, M. Takahashi, *Sens. Actuators, B,* 241 (2017) 1261.
26. A. K. Rivai, T. Kumagai, M. Takahashi, Prog. Nucl. Energy, 50 (2008) 575.
27. A. Iio, H. Ikeda, S. A. Anggraini, N. Miura, *Solid State Ionics*, 285 (2016) 234.
28. N. Miura, H. Jin, R. Wama, S. Nakakubo, P. Elumalai, V. V. Plashnitsa, *Sens. Actuators, B*, 152 (2011) 261.
29. S. H. Jensen, A. Hauch, P. V. Hendriksen, M. Mogensen, N. Bonanos and T. Jacobsen, *J. Electrochem. Soc.*, 154 (2007) 1325.
30. S. Raz, K. Sasaki, J. Maier and J. Riess, *Solid State Ionics*, 143 (2001) 181.
31. A. Jaccoud, C. Falgairette, G. Fóti and Ch. Comninellis, *Electrochim. Acta*, 52 (2007) 7927.
32. C. Falgairette, A. Jaccoud, G. Fóti and Ch. Comninellis, *J. Appl. Electrochem.*, 38 (2008) 1075.
33. N. Sakai, K. Yamaji, T. Horita, Y. P. Xiong, H. Kishimoto, M. E. Brito and H. Yokokawa, *Solid State Ionics*, 176 (2005) 2327.
34. J. O. Hirschfelder, R. B. Bird and E. L. Spotz, *Chem. Rev.*, 44 (1949) 205.
35. J. R. Welty, C. E. Wicks, R. E. Wilson and G. L. Rorrer, Fundamentals of momentum, heat, and mass transfer. 5th edition, John Wiley & Sons (2007).
36. P. W. Atkins, Physical Chemistry. 3rd edition, Oxford University Press, Oxford (1987).
37. D. M. Young and A. D. Crowell, Physical Adsorption of Gases. Butterworth, London (1962).